第 28 卷第 5 期 无 机 化 学 学 报 Vol.28 No.5
2012 年 5 月 CHINESE JOURNAL OF INORGANIC CHEMISTRY 1043-1049

多孔氧化铜空心微球的一步法制备及其光催化性能

邵 谦* 王小杰 葛圣松 王凌云 杨小琨
(山东科技大学化学与环境工程学院,青岛 266590)

摘要: 采用一步法成功制备出多孔氧化铜空心微球,用 SEM、XRD 和 FTIR 对制得的样品进行了表征。研究发现,碳源、反应温度、反应时间、$CuSO_4$ 浓度等实验条件在多孔微球的制备过程中起着重要作用。在实验结果的基础上,提出了多孔氧化铜空心微球的形成机理。制备的多孔氧化铜空心微球的比表面积为 409 $m^2 \cdot g^{-1}$,平均孔径为 3.15 nm,总孔体积为 0.256 $cm^3 \cdot g^{-1}$, 这种空心微球具有量子尺寸效应并对罗丹明 B 有较高的光催化性能。

关键词: CuO; 空心球; 金属氧化物; 催化性能
中图分类号: 0614.12 **文献标识码**: A **文章编号**: 1001-4861(2012)05-1043-07

Porous CuO Hollow Microspheres: One-Step Preparation and Photocatalytic Performance

SHAO Qian* WANG Xiao-Jie GE Sheng-Song WANG Ling-Yun YANG Xiao-Kun
(*College of Chemical and Environmental Engineering, Shandong University of Science & Technology, Qingdao, Shandong* 266590, *China*)

Abstract: Porous copper oxide (CuO) hollow microspheres were fabricated via a one-step method. The products were characterized by SEM, XRD and FTIR. The carbon source, hydrothermal temperature and time and the concentration of $CuSO_4$ play crucial roles in controlling the morphology of the title material. A formation mechanism was proposed based on the characterization results. The BET specific surface area of the hollow spheres is 409 $m^2 \cdot g^{-1}$, the average pore size is 3.15 nm, and the total pore volume is 0.256 $cm^3 \cdot g^{-1}$. The material exhibits a quantum size effect in UV spectrum and higher photocatalytic activity for degradation of rhodamine B (RhB) aqueous solution.

Key words: CuO; hollow microspheres; metal oxides; catalysis

0 Introduction

Hollow micro/nanostructures have recently become one of the hot research topics owing to their unique and superior performances. The hollow structures have high specific surface area and low density, and could be beneficial for application in the fields such as catalysis, photoelectricity, and biomedicine[1-3].

As an important p-type semiconductor, CuO has attracted a great deal of attention due to its promising application in catalysis [4], gas sensing [5], solar energy conversion [6], and lithium ion batteries as electrodes[7]. In recent years, a series of CuO nanomaterials with various morphologies have been obtained, such as spheres [8], flowers [9], nanowires [10], nanosheets and nanowhiskers [11], nanoplatelets [12], nanorods and branches [13], dandelions[14], and hollow structures[15-19], among which the hollow spheres exhibit unique performances. However, to the best of our knowledge,

收稿日期:2011-09-27。收修改稿日期:2011-12-28。
山东省科技攻关计划(No.2006GG2203022)资助项目。
*通讯联系人。E-mail:shaoqian01@126.com

the synthesis of porous CuO hollow microspheres via a facile hydrothermal method has not been reported.

The porous CuO hollow spheres were synthesized via a two-step method in our previous work[20], herein we report the preparation via a one-step method. The influence of hydrothermal temperature and time, and the concentration of $CuSO_4$ on the morphology of CuO structures were investigated. A formation mechanism was proposed based on the characterization results. Furthermore, the photocatalytic activity for the degradation of RhB was evaluated.

1 Experimental

1.1 Materials

Sucrose, glucose, copper sulfate pentahydrate ($CuSO_4 \cdot 5H_2O$) and absolute ethanol were purchased from Tianjin Bodi Co., Ltd. (Tianjin, China), and rhodamine B, from Shanghai Chemical Reagent Co., Ltd. (Shanghai, China). All the reagents were analytical grade and used without further purification. Distilled water was used in the experiments.

1.2 Preparation of porous CuO hollow microspheres

Sucrose was dissolved in 20 mL distilled water to form a clear 0.5 mol·L^{-1} solution followed by the addition of $CuSO_4 \cdot 5H_2O$. After ultrasonication for 30 min, the mixture was sealed in a 30 mL Teflon-lined autoclave and maintained at 160 ℃ for 16 h. The products were centrifuged and washed several times with distilled water and absolute ethanol, and then dried at 80 ℃ for 5 h. Finally, the products were calcined in air at 550 ℃ (heating rate of 3 ℃·min^{-1}) for 4 h.

1.3 Characterization

The phase of the products was determined by a Rigaku D/Max2500PC X-ray diffractometer (XRD) equipped with graphite monochromatized Cu $K\alpha$ radiation (λ =0.154 18 nm)under the following conditions: 30 kV as accelerating voltage; 100 mA as emission current; and the 2θ range of 5°~80° at a scan rate of 4°·min^{-1}.

The morphology was examined by a Beijing KYKY2800B scanning electron microscope (SEM) with an accelerating voltage of 10 kV. Fourier transform infrared (FTIR) spectra were recorded on a NICOLET 380 FTIR spectrometer using KBr pellet at room temperature in the region of 400~4 000 cm^{-1}. The BET specific surface area and the pore size distribution of the product were measured by a Beijing SSA-4300 pore size and surface area analyzer under the following conditions: Nitrogen as adsorption gas; the diameter range of 0.35~400 nm and the~pressure range of 0~120 kPa. The UV-Vis absorption spectrum of the product was recorded on a Shimadzu UV-2450 UV-Visible diffuse reflectance Spectrophotometer.

1.4 Photocatalytic activity test

The photocatalytic activity was evaluated by the photocatalytic decolorization of RhB aqueous solution performed at room temperature by dispersing 15 mg porous CuO hollow microspheres in 30 mL RhB aqueous solution of 10 mg·L^{-1}. The suspension was magnetically stirred in the dark for 30 min to ensure sufficient adsorption. A UV-light lamp with a wavelength of 254 nm was used as a light source. After UV-light irradiation for desired time, the reaction solution was filtered and the absorbance of the RhB aqueous solution was measured by a UV-Vis spectrophotometer (TU-1810, Beijing).

2 Results and discussion

2.1 Characterizations of the as-prepared samples

The SEM image of Cu-adsorbed carbon spheres synthesized at 160 ℃ for 16 h with 0.05 mol·L^{-1} $CuSO_4$ is shown in Fig.1a. The spheres are 5 to 6 μm in diameter. After calcination, hollow microspheres are with a diameter of ca. 15 μm (Fig.1b). The hollow cavity porous structure can be clearly observed from the broken spheres, as shown in Fig.1c. The thickness of the sphere shell is ca.1 μm. Note that the volume of the hollow microspheres expand after calcination. The broken hollow microspheres may be caused by the escaping of CO_2 during the calcination[21]. From Fig.1d, the surface of the sphere is composed of aggregated irregular nano-polyhedra of copper oxides, yielding an inherent porosity of the shell.

The XRD patterns of the Cu-adsorbed carbon

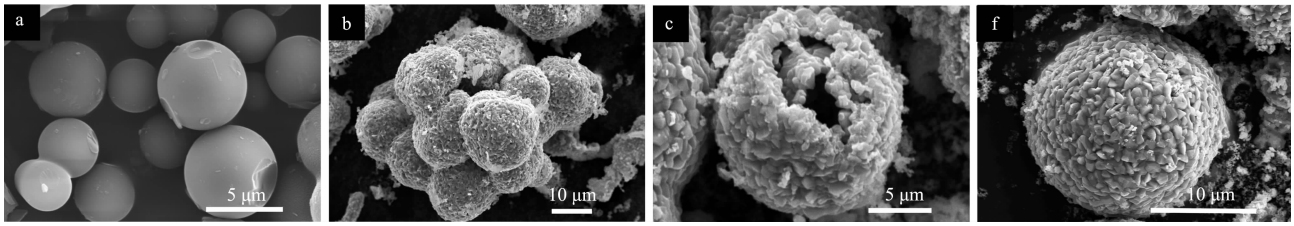

(a) Hydrothermally treated sucrose/Cu^{2+}mixtures before calcinations; (b) porous CuO hollow mirospheres after calcinations; (c) an individual broken microsphere; (d) an individual intact microsphere

Fig.1　SEM images of the products

spheres before calcination and the porous CuO hollow microspheres obtained after calcination are shown in Fig.2. From Fig.2a, the peaks correspond to face-centered cubic (fcc) structure of metal copper due to the reduction of Cu^{2+} by glucose under the hydrothermal conditions. After calcination (Fig.2b), most of the diffraction peaks can be indexed to the monoclinic phase CuO (PDF No.48-1548). Meanwhile, a weak peak of cubic Cu_2O is also detected owing the reduction of Cu^{2+} to Cu^{+} under the hydrothermal conditions. The crystallite size calculated by Jade is 34.7 nm.

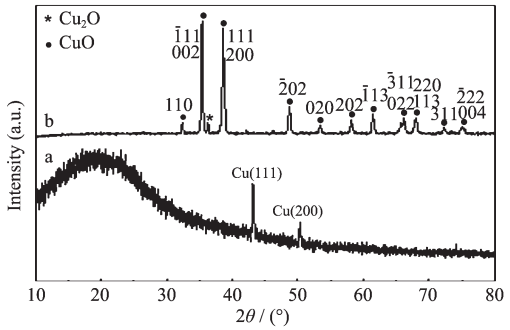

Fig.2　XRD patterns of the products before (a) and after (b) calcination

Fig.3 shows the FTIR spectra of the Cu-adsorbed carbon spheres before calcination and the porous CuO hollow microspheres obtained after calcination. From Fig.3a, the band at 3 387 cm^{-1} is the stretching vibration of the hydroxyls of adsorbed water, the ones at 1 699 and 1 610 cm^{-1} are attributed to C=O and C=C vibrations, respectively. The peaks in the range of 1 300~1 000 cm^{-1} include the C-OH stretching and OH bending vibrations. After calcination, the bands in the range of 2 000~1 000 cm^{-1} become very weak (Fig.3b), indicating that most of the carbon spheres

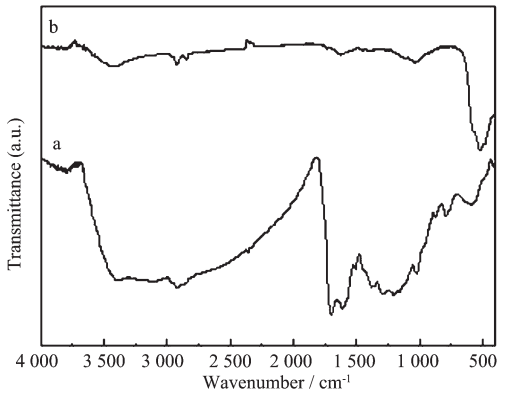

Fig.3　FTIR spectra of the products before (a), and after (b) calcination

are removed. The IR peak observed at 528 cm^{-1} is assigned to the Bu mode of monoclinic CuO[22].

The chemical compositions of the product were analyzed by EDS. There are two kinds of peaks in the EDS spectra (Fig.4), which indicates the presence of Cu and O element and the atomic% of C is 8.4. It can be inferred that most of the carbon spheres are removed.

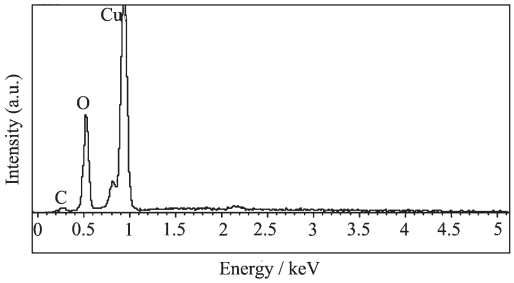

Fig.4　EDS spectrum of the porous CuO hollow microspheres

The nitrogen adsorption-desorption isotherm and the pore size distribution plots of porous CuO hollow microspheres are shown in Fig.5. According to the IUPAC classification, the nitrogen adsorption and

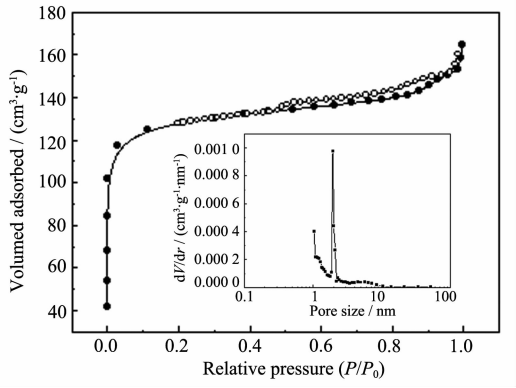

Fig.5 Nitrogen adsorption-desorption isotherms and the BJH pore size distribution (inset) of the porous CuO hollow microspheres

desorption isotherm of the microspheres is characteristic of the type Ⅱ isotherm with a type H3 hysteresis loop. On the basis of the nitrogen adsorption-desorption results, the porous CuO hollow microspheres exhibit a BET surface area of 409 $m^2 \cdot g^{-1}$ and a total pore volume (r=173 nm, P/P_0=0.994) of 0.256 $cm^3 \cdot g^{-1}$. The pore-size distribution was calculated from the desorption data, as shown in the inset of Fig.5. The average pore size is 3.15 nm. Besides the pores in the range of 1~100 nm measured by BJH method, some macropores larger than 100 nm can also be observed from the SEM image (Fig.1d).

Fig.6 shows the UV absorption spectrum of the porous CuO hollow microspheres. There is a sharp absorption peak centered at ca. 212 nm, which considerably blue-shifted from the value of 303 nm reported by Qian et al[12]. The blue-shift is possibly as a result of quantum size effects, owing to the irregular

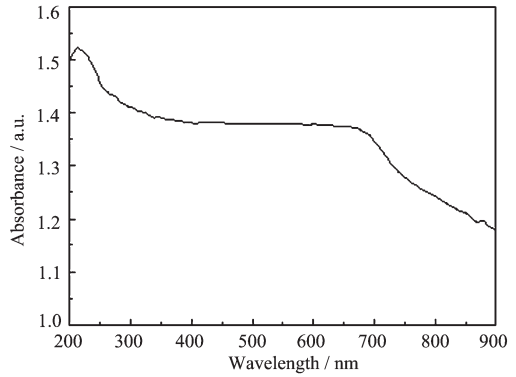

Fig.6 UV absorption spectrum of the porous CuO hollow microspheres

nano-polyhedra covered on the face of the microspheres[23].

2.2 Influencing factors

The influence of carbon source on the size and morphology of the products was investigated in the presence of 0.05 $mol \cdot L^{-1}$ $CuSO_4$ at 160 ℃ for 8 h. From Fig.7a, besides the hollow spheres, a large number of hollow tubes are observed. It can be presumed that the tubes are essentially generated by a synergistic reduction/carbonization process, as elucidated for Ag nanocables[24]. To avoid such redox reactions during the carbonization of carbohydrate, glucose is replaced with non-reducing sucrose as the precursor. After hydrothermal treatment with sucrose for 8 h, porous CuO hollow microspheres are obtained (Fig.7b).

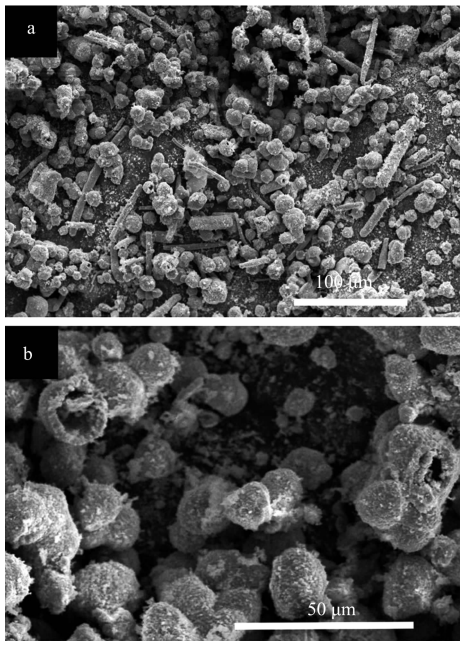

(a) glucose; (b) sucrose

Fig.7 SEM images of the CuO products obtained with different carbon sources

The effect of hydrothermal time on the size and morphology of the products was studied in the presence of 0.05 $mol \cdot L^{-1}$ $CuSO_4$ and sucrose at 160 ℃. After hydrothermal treatment for 8 h, porous CuO hollow microspheres with the diameter of ca. 13 μm are obtained (Fig.8a). When the hydrothermal time is extended to 16 h, the porous CuO hollow microspheres are about 15 μm in diameter (Fig.8b).

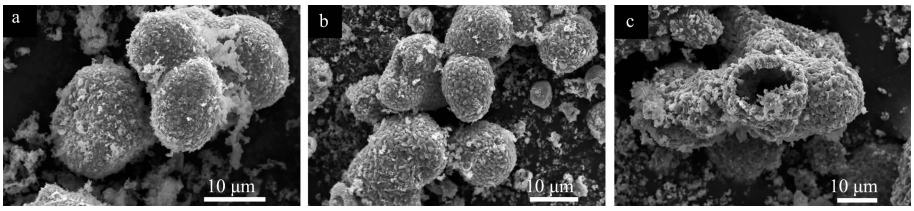

(a) 8 h; (b) 16 h; (c) 24 h

Fig.8　SEM images of the CuO products obtained for various periods of time

Further extending the hydrothermal time to 24 h results in the formation of irregular and imperfect spheres(Fig.8c).

Hydrothermal temperature is a crucial factor on the formation of porous CuO hollow microspheres. Porous CuO hollow microspheres could be obtained in the temperature range of 140~160 ℃(Fig.9). However, when the temperature is lower than 120 ℃, no products can be obtained.

The concentration of $CuSO_4$ also plays an essential role in controlling the morphology of the products. Porous CuO hollow microspheres could be obtained at a concentration of 0.05 mol·L^{-1} (Fig.10a). Nevertheless, when the concentration is increased to 0.1 mol·L^{-1} and 0.2 mol·L^{-1}, a lot of pieces are formed with only a few large spheres (Fig.10b and Fig. 10c). The pieces might result from the broken spheres owing to the escaping of a large amount of CO_2 during the calcination.

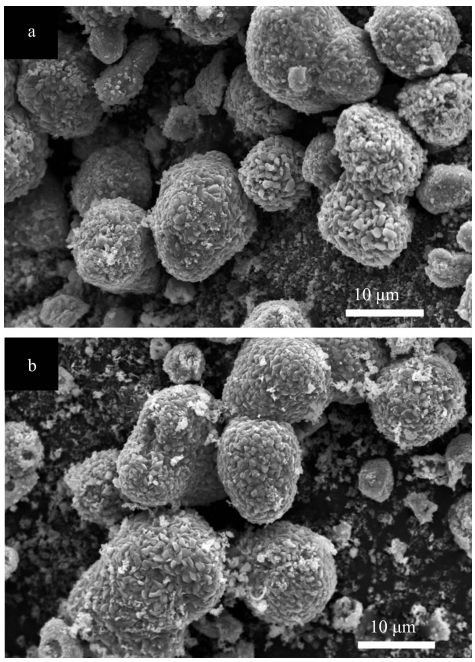

(a) 140 ℃; (b) 160 ℃

Fig.9　SEM images of the porous CuO hollow microspheres obtained at different hydrothermal temperatures

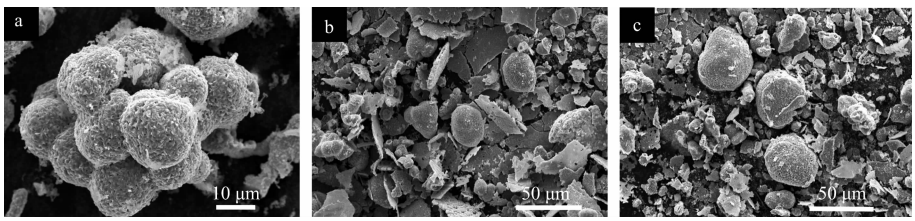

(a) 0.05 mol·L^{-1}; (b) 0.1 mol·L^{-1}; (c) 0.2 mol·L^{-1}

Fig.10　SEM images of the CuO products obtained with different $CuSO_4$ concentrations

2.3　Formation mechanism

The formation mechanism of the porous CuO hollow microspheres is proposed in Fig.11. Oligosaccharides molecules are firstly formed from sucrose by polymerization under the hydrothermal conditions. When the solution reaches a critical supersaturation, a short single burst of nucleation is produced. This carbonization step may arise from cross-linking induced by intermolecular dehydration of linear or branchlike oligosaccharides[25]. The surface of the spheres is hydrophilic and has a distribution of -OH and C=O groups. During the growth of carbon spheres, the functional groups bind with copper ions through coordination or electrostatic interactions. During the subsequent calcination, carbon spheres are removed, and the Cu-adsorbed layers became denser

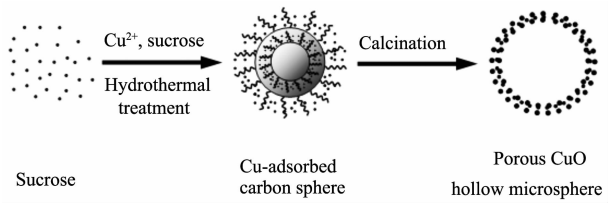

Fig.11 Scheme for the formation of porous CuO hollow microspheres

and cross-linked. With the escaping of CO_2, the volume of the hollow microspheres expanded after calcination.

2.4 Photocatalytic activity

Fig.12 shows the UV absorption spectra of the RhB solution with the porous CuO hollow microspheres as the catalyst under UV irradiation at 254 nm. The absorption peak intensity decreases with increasing the irradiation time. Fig.13 shows the curves between the degradation ratio and irradiation time with and without the micrpspheres. In 90 min, the degradation ratio of RhB is only 25.4% under the UV irradiation without the catalyst, and the ratio increases to 96% using the porous CuO hollow microspheres as the catalyst. Due to the large specific surface area and more capacious interspaces, the porous CuO hollow microspheres can provide more active sites for the photocatalytic degradation of RhB molecules[18].

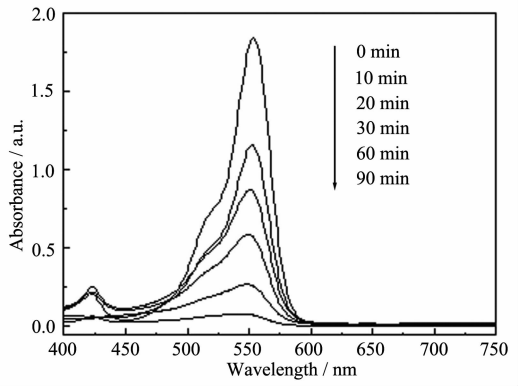

Fig.12 UV absorption spectra of the different RhB solutions in the presence of porous CuO microspheres under UV irradiation

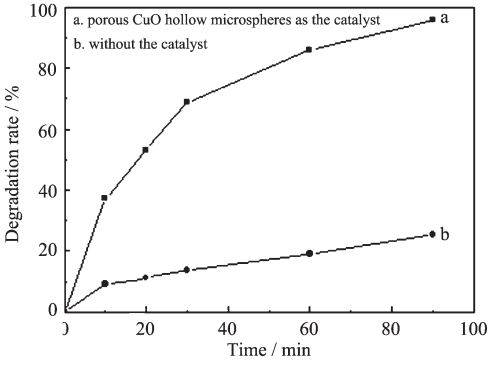

(a) porous CuO hollow microspheres as the catalyst; (b) without the catalyst

Fig.13 Degradation rate of RhB vs irradiation time

3 Conclusions

Porous copper oxide hollow microspheres with higher specific surface area were fabricated under hydrothermal conditions. Carbon source, hydrothermal temperature and time, and the concentration of $CuSO_4$ could influence the morphology of the final products. The formation mechanism of porous CuO hollow microspheres is proposed. The porous CuO hollow microspheres exhibit higher photocatalytic activity for degradation of RhB aqueous solution under UV irradiation.

Acknowledgements: This work was financially supported by Programs for Science and Technology Development of Shandong Province (Grant No. 2006GG2203022).

References:

[1] Ma Y R, Qi L M. *J. Colloid Interface Sci*., **2009**,**335**:1-10
[2] An K, Hyeon T. *Nano Today*, **2009**,**4**:359-373
[3] Zhao Y, Jiang L. *Adv. Mater*., **2009**,**21**:3621-3638
[4] Hong J M, Li J, Ni Y H. *J. Alloys Compd.*, **2009**,**481**:610-615
[5] Zhang J T, Liu J F, Peng Q, et al. *Chem. Mater.*, **2006**,**18**:867-871
[6] Anandan S, Wen X G, Yang S H. *Mater. Chem. Phys*., **2005**, 93:35-40
[7] Ke F S, Huang L, Wei G Z, et al. *Electrochim.*, **2009**,**54**:5825-5829
[8] Song H C, Park S H, Huh Y D. *Bull. Korean Chem*., **2007**, **28**:477-480
[9] Vaseem M, Umar A, Kim S H, et al. *J. Phys. Chem.*, **2008**, **112**:5729-5735
[10]Huang C Y, Chatterjee A, Liu S B, et al. *Appl. Surf. Sci.*, **2010**,**256**:3688-3692

[11]Wang W W, Zhu Y J, Cheng G F, et al. *Mater. Lett.*, **2006**, 60:609-612

[12]Zou G F, Li H, Zhang D W, et al. *J. Phys. Chem.*, **2006**, **110**:1632-1637

[13]Xiao H M, Fu S Y, Zhu L P, et al. *Eur. J. Inorg. Chem.*, **2007**,**14**:1996-1971

[14]Zhang Z P, Shao X Q, Yu H D, et al. *Chem. Mater.*, **2005**, **17**:332-336

[15]Zhang Y G, Wang S T, Qian Y T, et al. *Solid State Sci.*, **2006**,**8**:462-466

[16]Zhang Y, He X L, Li J P, et al. *Sens. Actuators B*, **2007**,**128**:293-298

[17]Gao S Y, Yang S X, Shu J, et al. *J. Phys. Chem. C*, **2008**, **112**:19324-19328

[18]Wang S L, Xu H, L Qian Q, et al. *J. Solid State Chem.*, **2009**,**182**:1088-1093

[19]Yu H G, Yu J G, Liu S W, et al. *Chem. Mater.*, **2007**,**19**: 4327-4334

[20]Shao Q, Wang X J, Liu Q Y, et al. *J. Nanosci. Nanotechnol.*, DOI:10.1166/jnn.**2011**.5005

[21]Zhao W W, Liu Y, Li H L, et al. *Mater. Lett.*, **2008**,**62**:772-774

[22]Kliche G, Popovic Z V. *Phys. Rev. B*, **1990**,**42**:10060-10066

[23]Ge S S, Wang Q Y, Li J Y, et al. *J. Alloys Compd.*, **2010**, **494**:169-174

[24]Yu S H, Cui X J, Li L L, et al. *Adv. Mater.*, **2004**,**6**:1636-1640

[25]Sun X M, Li Y D. *Angew. Chem. Int. Ed.*, **2004**,**3**:597-601